NATIONAL ADVISORY COMMITTEE FOR AERONAUTICS

TECHNICAL NOTE 2019

PENETRATION OF AIR JETS ISSUING FROM CIRCULAR, SQUARE, AND ELLIPTICAL ORIFICES DIRECTED PERPENDICULARLY TO AN AIR STREAM

By Robert S. Ruggeri, Edmund E. Callaghan
and Dean T. Bowden

Lewis Flight Propulsion Laboratory
Cleveland, Ohio

NACA
Washington
February 1950

NATIONAL ADVISORY COMMITTEE FOR AERONAUTICS

TECHNICAL NOTE 2019

PENETRATION OF AIR JETS ISSUING FROM CIRCULAR, SQUARE, AND ELLIPTICAL ORIFICES DIRECTED PERPENDICULARLY TO AN AIR STREAM

By Robert S. Ruggeri, Edmund E. Callaghan
and Dean T. Bowden

SUMMARY

An experimental investigation was conducted to determine the penetration of air jets directed perpendicularly to an air stream. Jets issuing from circular, square, and elliptical orifices were investigated and the jet penetration at a position downstream of the orifice was determined as a function of jet density, jet velocity, air-stream density, air-stream velocity, effective jet diameter, and orifice flow coefficient. The jet penetrations were determined for nearly constant values of air-stream density at three tunnel-air velocities and for a large range of jet velocities and densities. The results were correlated in terms of dimensionless parameters and the penetrations of the various shapes were compared.

Greater penetration was obtained with the square orifices and the elliptical orifices having an axis ratio of 4:1 at low tunnel-air velocities and low jet pressures than for the other orifices investigated. The square orifices gave the best penetrations at the higher values of tunnel-air velocity and jet total pressure.

INTRODUCTION

A circular jet directed perpendicularly to an air stream can be satisfactorily utilized as a means of heating or cooling an air stream (reference 1). A later investigation (reference 2) showed that square and elliptical orifices give higher flow coefficients than circular orifices. Better penetrations might therefore be obtained with orifice shapes other than circles. In addition, a large variation of flow coefficient with jet-pressure ratio was observed in the investigation reported in reference 2. It is possible that better correlation of the data of reference 1 could be obtained by including the flow coefficient in the analysis of the data presented therein.

An investigation to determine the penetration of air jets issuing from circular, square, and elliptical orifices was undertaken in a 2- by 20-inch-duct tunnel at the NACA Lewis laboratory, and a study of the effect of variations in the orifice flow coefficient on the correlation of the experimental data was made. The jet penetration at a fixed position downstream of the orifices was determined at tunnel-air velocities of 160, 275, and 380 feet per second for circular, square, and elliptical orifices. Each orifice was investigated over a range of pressure ratios from 1.15 to 3.2 and at a jet total temperature of approximately 400° F.

APPARATUS AND PROCEDURE

The orifices investigated consisted of three circles, two squares, two ellipses with an axis ratio of 4:1, and two ellipses with an axis ratio of 2:1. The circular orifices had diameters of 0.375, 0.500, and 0.625 inch; the squares and the ellipses had areas equivalent to the 0.375- and 0.625-inch-diameter circles. For these investigations, the elliptical orifices were mounted with the major axis parallel to the air stream and the square orifices with two edges parallel to the air stream. A boundary-layer bypass was employed in order to minimize the effect of tunnel boundary layer. Air for the jets was obtained by passing high-pressure air through an electric heater and into a plenum chamber, the upper wall of which contained the orifices (fig. 1).

Each orifice was investigated over a range of orifice-pressure ratios from 1.15 to 3.2 for a jet total temperature of approximately 400° F, and at tunnel-air velocities of 160, 275, and 380 feet per second. The penetration of each jet was measured at the farthest position downstream of the orifice center line (18.88 in.) with a rake consisting of 22 thermocouple probes spaced $\frac{1}{2}$ inch apart. Static pressures were measured in the plane of the orifice and at a point upstream of the orifice by pressure taps in the tunnel wall.

SYMBOLS

The following symbols are used in this report:

C flow coefficient, ratio of measured to theoretical flow

D_j diameter of circular jet orifice, feet

l depth of jet penetration into air stream at distance s downstream of orifice center line, feet

s	mixing distance or distance downstream of orifice center line, feet
V_j	velocity of jet at vena contracta, feet per second
V_0	velocity of free stream, feet per second
w	duct width, feet
μ_j	viscosity of jet at vena contracta, slugs per foot-second
μ_0	viscosity of free-stream air, slugs per foot-second
ρ_j	mass density of jet at vena contracta, slugs per cubic foot
ρ_0	mass density of free-stream air, slugs per cubic foot

RESULTS AND DISCUSSION

The analysis of reference 1 indicates that the penetration coefficient l/D_j can be correlated in terms of the jet Reynolds number $(\rho_j V_j D_j)/\mu_j$, the velocity ratio V_j/V_0, the density ratio ρ_j/ρ_0, the viscosity ratio μ_j/μ_0, the mixing distance-diameter ratio s/D_j, and the width coefficient w/D_j. Depth of penetration, defined in reference 1 as the point at which the temperature is 1° F above the free-stream total temperature, was obtained from the temperature profiles measured at the thermocouple rake.

The primary factors in the correlation of the penetration data are density ratio, velocity ratio, and mixing distance-diameter ratio, as indicated by the results of reference 1. The effect of the other parameters was not evident because no consistent trends could be observed in the data. Appreciable over-all scatter of the data, however, indicated that not all the necessary variables were included in the analysis. The analysis of reference 1 does not include an effect of jet Mach number, that is, pressure ratio. The scatter evident in reference 1 may be caused in part by the variation of flow coefficient with pressure ratio shown in reference 2. In addition to the effect of jet Mach number on the flow coefficient noted in reference 2, a small effect of jet Reynolds number on the flow coefficient was observed as well as a small effect of width coefficient on the jet flow.

The inclusion of the flow coefficient in the analysis might eliminate much of the data scatter already discussed by including in part some effect of jet Mach number, jet Reynolds number, and width coefficient. Because the flow coefficient is the ratio of the actual flow to the theoretical flow, it may also be considered as a ratio of the effective jet area to the geometric orifice area. The effective jet diameter is therefore related to the geometric diameter by the square root of the flow coefficient.

In order to investigate the effect of flow coefficient on the data correlation, a plot similar to that in reference 1 was made of the penetration coefficient as a function of the product of the density ratio, the velocity ratio, and the square root of the mixing distance-diameter ratio (fig. 2). The flow coefficients were then calculated by the methods presented in reference 2 and the data in figure 2 were replotted (fig. 3), with the effective jet diameter $\sqrt{C}\,D_j$ replacing the actual jet diameter D_j in the parameters. A comparison of figures 2 and 3 indicates that the scatter has been reduced by using the flow coefficient in the correlation. It is therefore evident that the correlation is improved when the actual jet diameter is replaced by the effective jet diameter. Hereinafter the penetration coefficient and mixing distance-diameter ratio are based on the effective jet diameter and are redefined as $l/\sqrt{C}\,D_j$, and $s/\sqrt{C}\,D_j$, respectively.

The analysis of the penetrations obtained with the square orifices was conducted in a manner similar to that employed for circular orifices. The penetration coefficient was first plotted as a function of the product of the density ratio and the velocity ratio. For each square orifice, the penetration coefficient was based on the diameter of the equivalent-area circle and in both cases single curves were obtained. Because the two curves for the square orifices were similar to those obtained for the circles of the same area, the penetration coefficients for both square orifices were plotted as a function of the product of the density ratio, the velocity ratio, and the square root of the mixing distance-diameter ratio (fig. 4); as for the circular-orifice data, a single curve was obtained. A comparison of figures 3 and 4 shows that slightly higher penetration coefficients were obtained with square orifices than with circular orifices.

A similar procedure was first employed in the correlation of the data obtained with the elliptical orifices. A plot was made of the penetration coefficient as a function of the product of the density ratio and the velocity ratio using a penetration coefficient based on the equivalent-area circle. Results obtained with the ellipse having an axis ratio of 4:1 and an area equivalent to a

0.375-inch-diameter circle are shown in figure 5. Three separate curves dependent on the tunnel-air velocity were obtained. Further analysis of these data showed that correlation could be obtained provided the penetration coefficient was plotted as a function of the product of the density ratio and the square of the velocity ratio, as shown in figure 6. The data for the 0.625-inch equivalent-diameter ellipse with an axis ratio of 4:1 were then plotted in terms of the same parameters and again a single curve was obtained (fig. 6). Comparison shows that the curves in figure 6 are separated by a function of the equivalent diameter. Because of the shape of the curves at the lower values of the parameter and because they become approximately parallel at the higher values of the parameter, it is not possible to correlate the data for both ellipses in terms of the ratio of mixing distance to diameter and obtain a single curve. It should be possible, however, to interpolate between the two curves and obtain values at other ratios of mixing distance to diameter s/D_j.

In the analysis of data for the ellipses with an axis ratio of 2:1, the procedure followed was similar to that employed with the ellipses having an axis ratio of 4:1. In order to correlate the penetration coefficients at all tunnel-air velocities, the penetration coefficient was plotted as a function of the product of the density ratio and the velocity ratio raised to the 1.5 power. Use of this parameter made possible the correlation of the data for the ellipses with an axis ratio of 2:1 (fig. 7). As for the ellipses having an axis ratio of 4:1, the nature of the curves precludes further correlation in terms of the ratio of mixing distance to diameter and again it is necessary to interpolate between the curves to obtain values at other ratios of mixing distance to diameter.

A study of the parameters required for correlating the data of the circles and the ellipses with axis ratios of 2:1 and 4:1 showed that the power to which the velocity ratio was raised increased with increasing axis ratio. Velocity-ratio exponent is shown as a function of axis ratio in figure 8. The curve indicates that the rate of increase of the velocity-ratio exponent decreased with increasing axis ratio. Further study of figure 8 indicates that an ellipse turned at right angles to the air stream may require exponents less than 1.0 because the effective aspect ratio with respect to the air stream is less than 1.0.

Because boundary-layer removal was employed throughout the investigation, the effect of boundary-layer thickness on jet penetration was not determined. From the correlation of the data, however, the effect appears to be small. The low momentum of the boundary layer enables the high-velocity jet to penetrate the layer almost

unaffected. Hence, a very thick boundary layer might add slightly to the penetration because the jet is farther from the surface when it enters the free stream of high momentum.

Because the ellipses do not correlate in terms of the same parameters used for the circles and the squares, no direct comparison of all the shapes can be obtained, except for specific values of jet total pressure, jet total temperature, tunnel-air velocity, and tunnel total pressure.

The calculated penetration of the four shapes at assumed tunnel-air velocities of 150, 250, and 350 feet per second as a function of jet total pressure is shown in figures 9(a), 9(b), and 9(c), respectively. These curves were calculated using the curves of figures 3, 4, 6, and 7 and assuming a free-stream total pressure of 29.92 inches of mercury, a free-stream total temperature of 59° F, and a jet total temperature of 400° F.

A study of figure 9 shows that in general at the low tunnel-air velocities the squares and the ellipses with an axis ratio of 4:1 gave the best penetration (fig. 9(a)) and at the high tunnel-air velocities and jet pressures the squares gave the best penetrations (figs. 9(b) and 9(c)). In general, if the specific conditions of jet total pressure, jet total temperature, air-stream velocity, and air-stream total pressure are known, it is best to calculate the necessary parameters and to compare the penetration coefficients before selecting a particular orifice shape.

SUMMARY OF RESULTS

The following results were obtained from an investigation to determine the penetration of air jets issuing from circular, square, and elliptical orifices directed perpendicularly to an air stream:

1. The use of the flow coefficient to obtain an effective jet diameter provided better correlation of the penetration coefficients of circular orifices in terms of the usual parameters of density ratio, velocity ratio, and mixing distance-diameter ratio.

2. The penetration coefficients obtained with square orifices could be correlated with the same parameter used for the circles, provided that a jet dimension equal to the diameter of the equivalent-area circle was used.

3. It was possible to correlate the ellipse data in terms of the product of the density ratio and the velocity ratio raised to a power. The power to which the velocity ratio must be raised for correlation increased with increasing axis ratio.

4. Greater penetrations were obtained with square orifices than with circular orifices of equal area.

5. At low tunnel airspeeds and low jet pressures greater penetration was obtained with the square orifices and the elliptical orifices having an axis ratio of 4:1 than with the other orifices investigated. The square orifices gave the best penetrations at the higher values of tunnel-air velocity and jet total pressure.

Lewis Flight Propulsion Laboratory,
National Advisory Committee for Aeronautics,
Cleveland, Ohio, September 27, 1949.

REFERENCES

1. Callaghan, Edmund E., and Ruggeri, Robert S.: Investigation of the Penetration of an Air Jet Directed Perpendicularly to an Air Stream. NACA TN 1615, 1948.

2. Callaghan, Edmund E., and Bowden, Dean T.: Investigation of Flow Coefficient of Circular, Square, and Elliptical Orifices at High Pressure Ratios. NACA TN 1947, 1949.

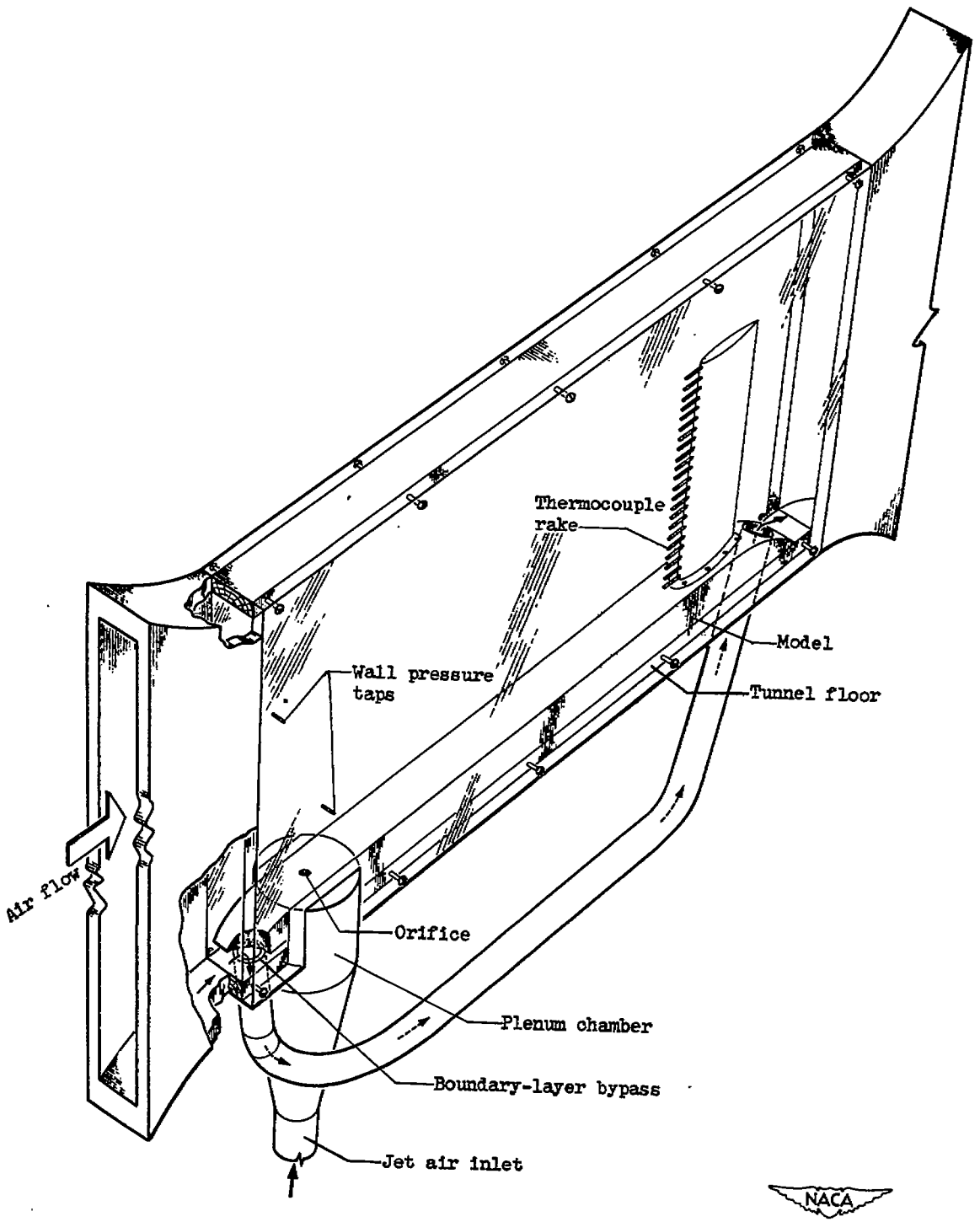

Figure 1. - Arrangement of orifice in plane parallel to air stream.

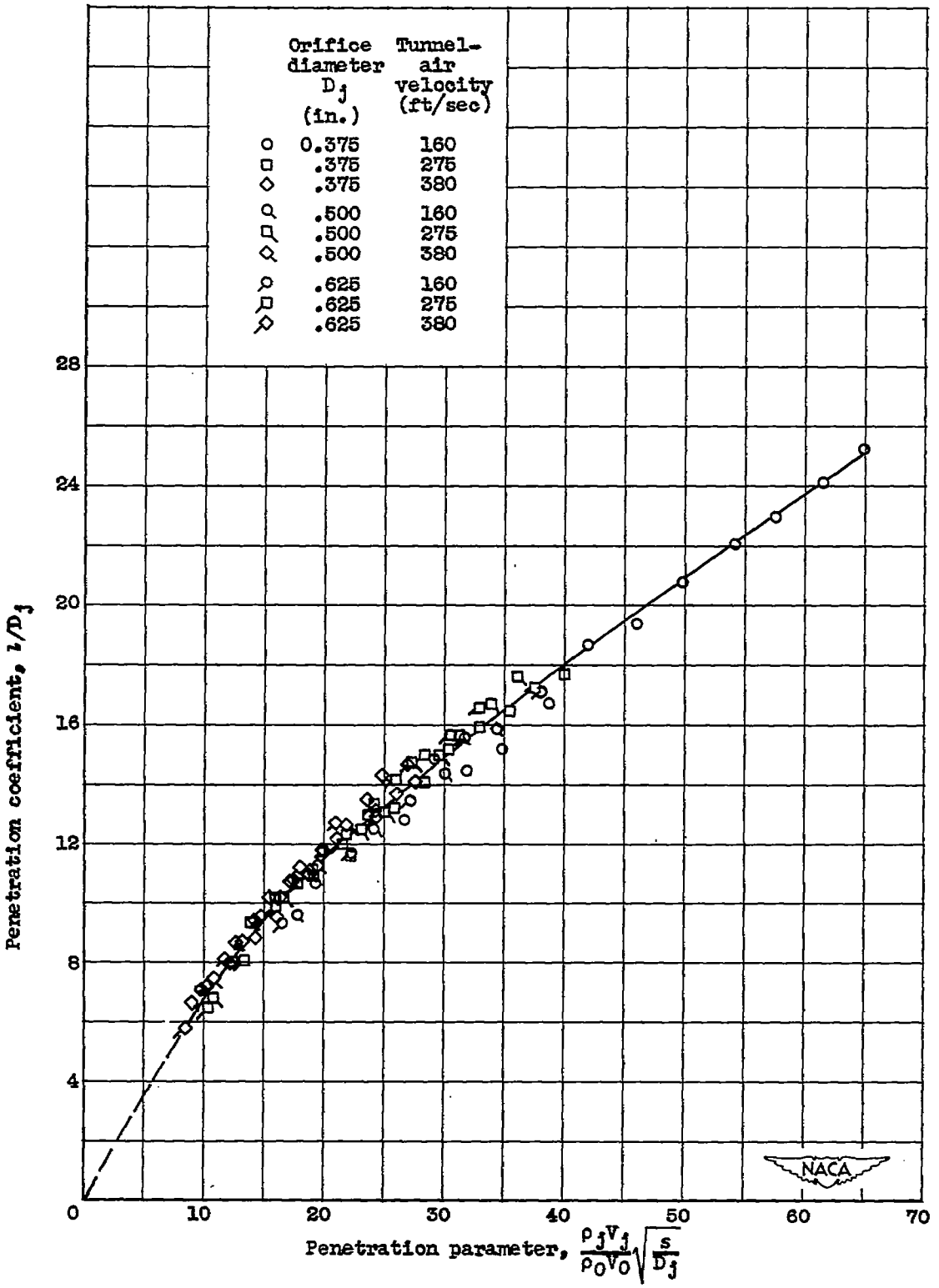

Figure 2. - Variation of penetration coefficient l/D_j with penetration parameter $\frac{\rho_j V_j}{\rho_0 V_0}\sqrt{\frac{s}{D_j}}$ for circular orifices.

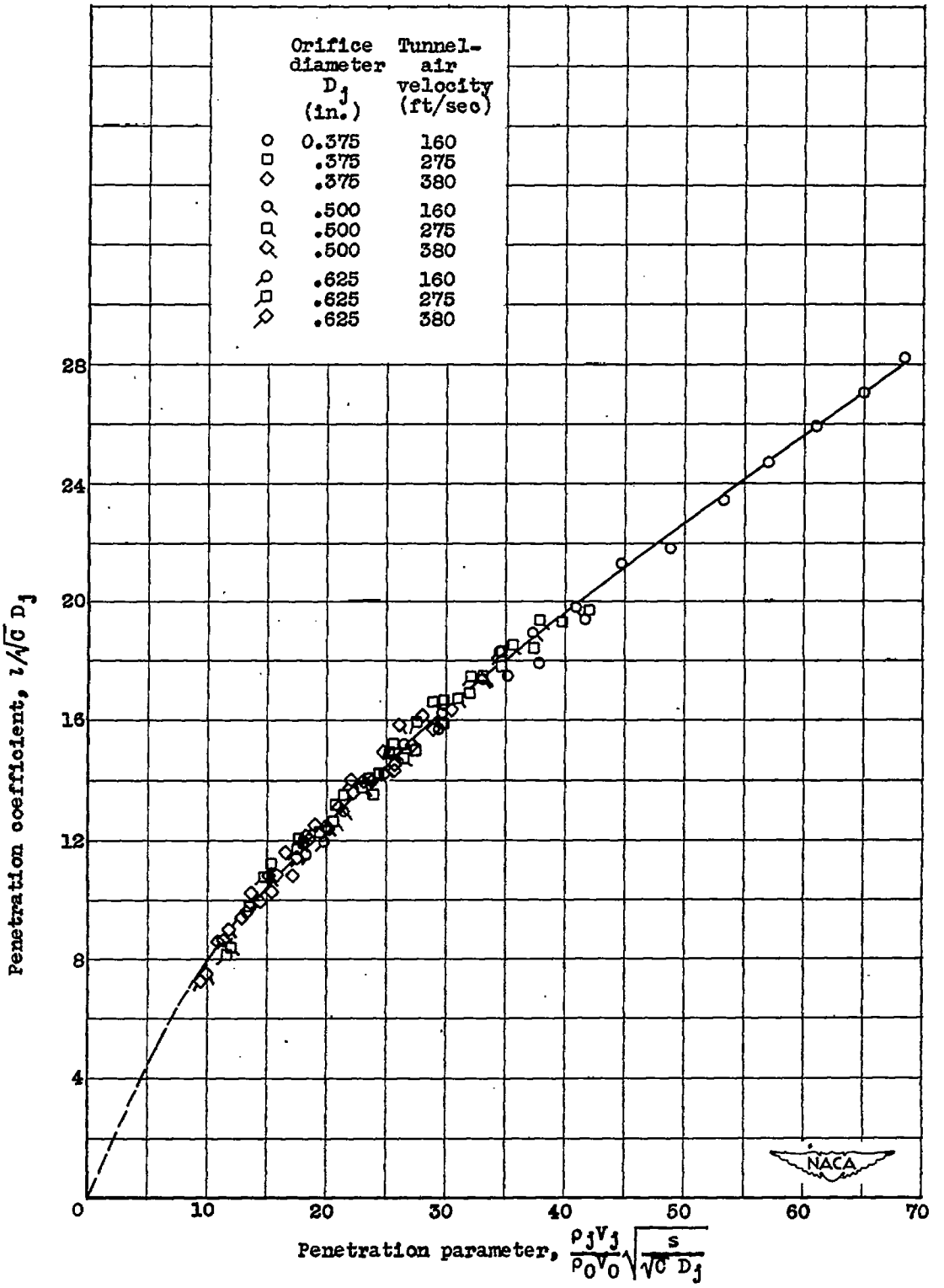

Figure 3. - Variation of penetration coefficient $l/\sqrt{C}\,D_j$ with penetration parameter $\frac{\rho_j V_j}{\rho_0 V_0}\sqrt{\frac{s}{\sqrt{C}\,D_j}}$ for circular orifices.

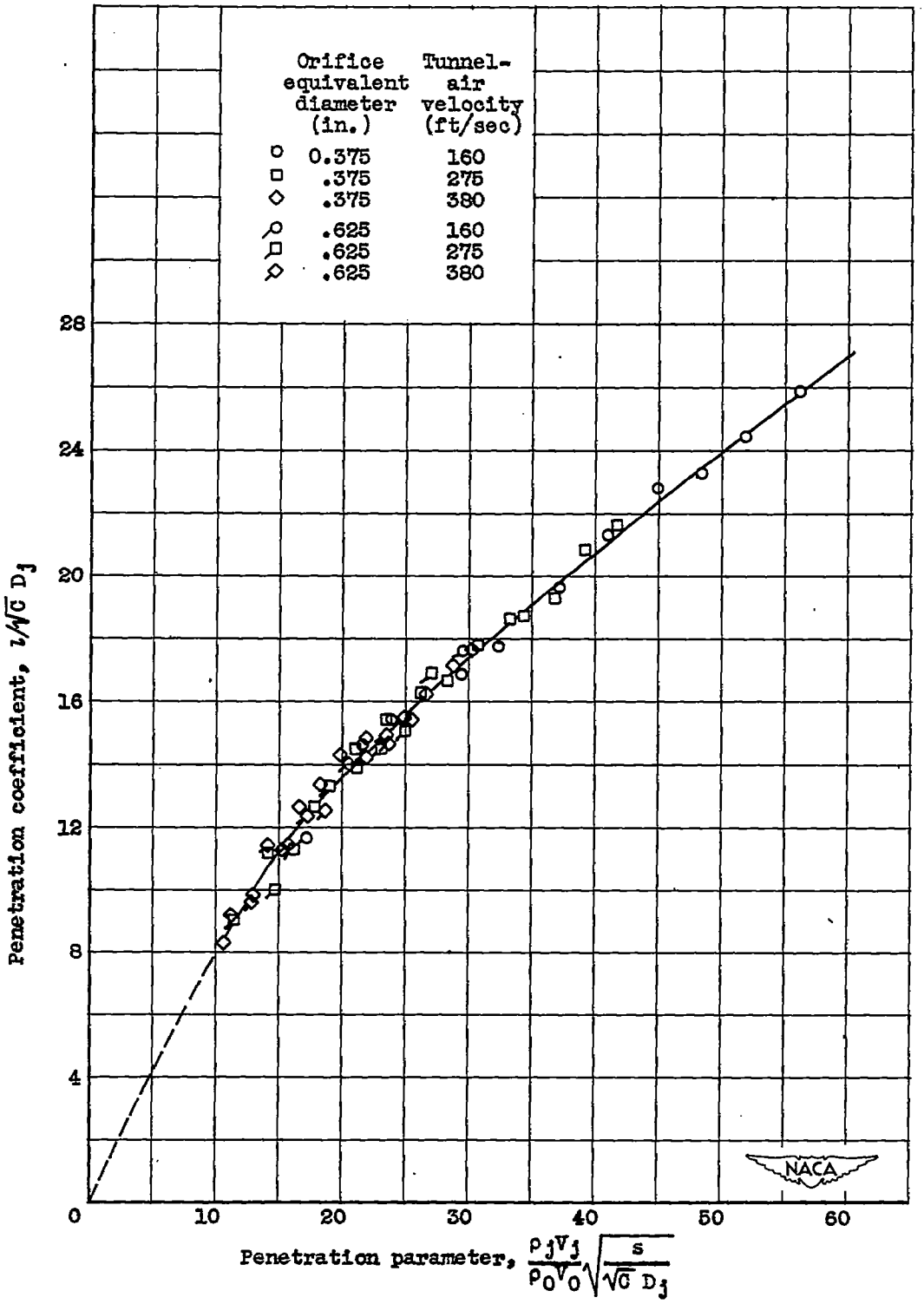

Figure 4. - Variation of penetration coefficient $l/\sqrt{C}\,D_j$ with penetration parameter $\frac{\rho_j V_j}{\rho_0 V_0}\sqrt{\frac{s}{\sqrt{C}\,D_j}}$ for square orifices.

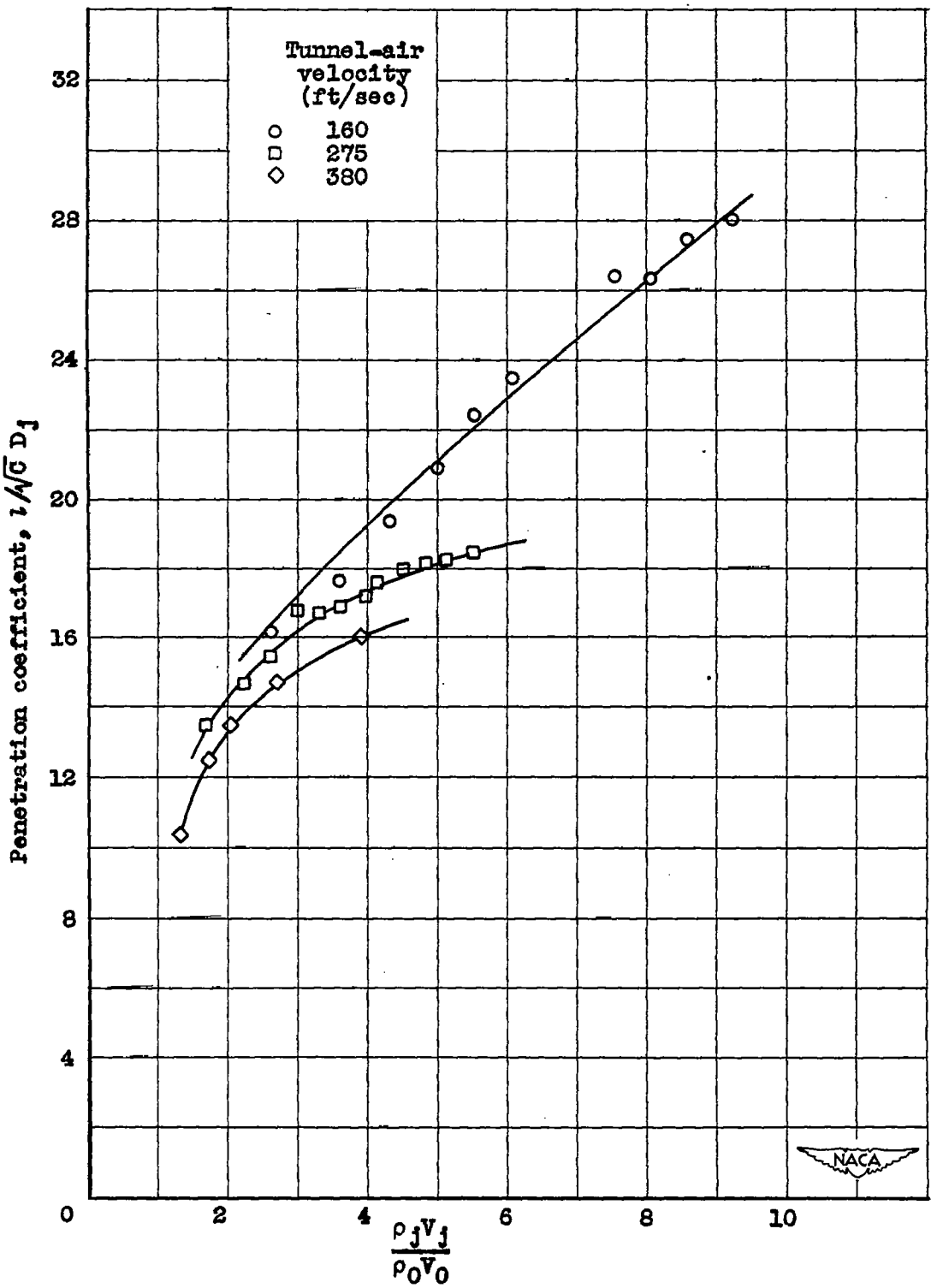

Figure 5. - Variation of penetration coefficient $l/\sqrt{C}\,D_j$ with $\frac{\rho_j V_j}{\rho_0 V_0}$ for 0.375-inch equivalent-diameter ellipse with an axis ratio of 4:1. Ratio of mixing distance to diameter s/D_j, 50.3.

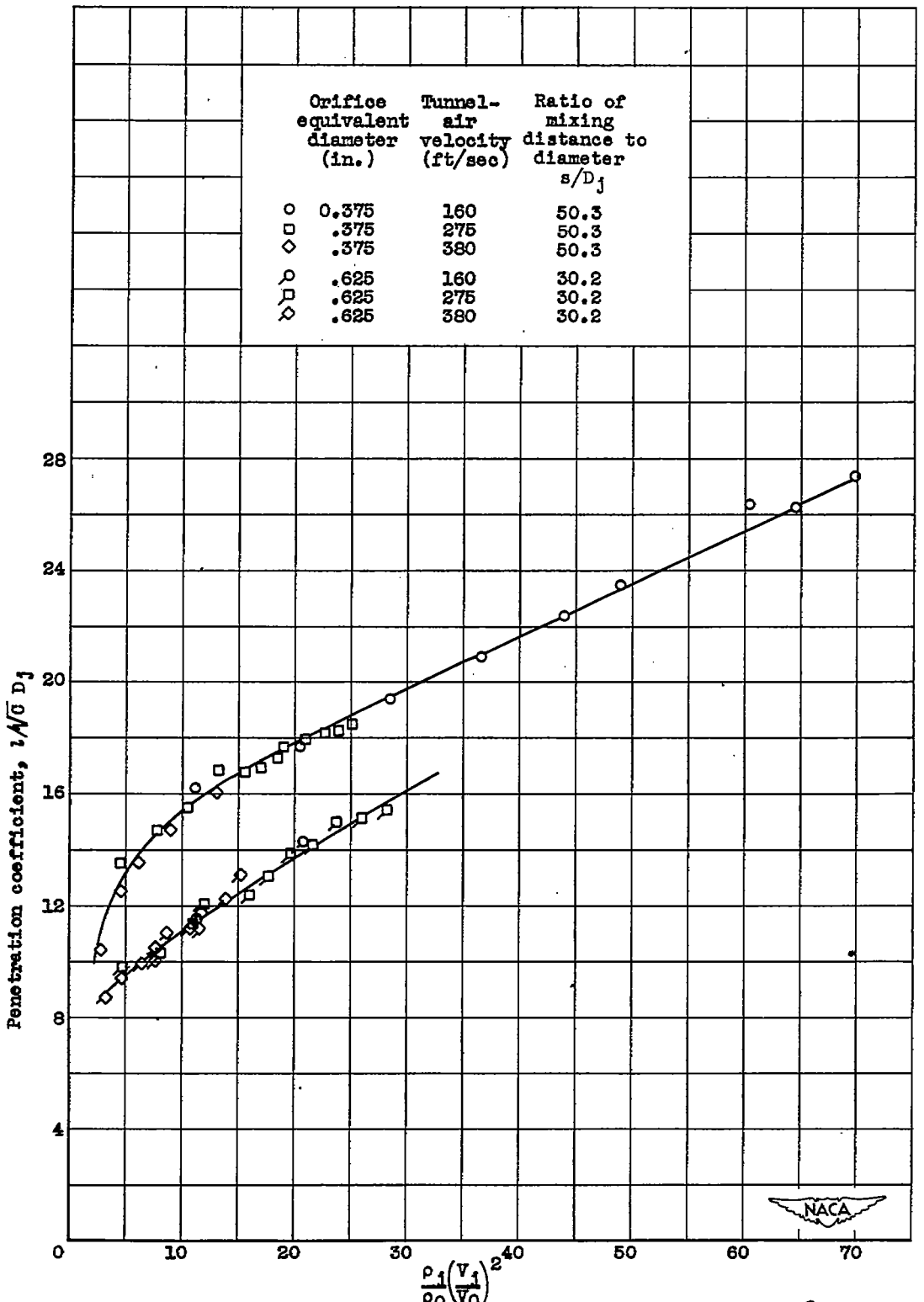

Figure 6. - Variation of penetration coefficient $l/\sqrt{C}\,D_j$ with $\frac{\rho_j}{\rho_0}\left(\frac{V_j}{V_0}\right)^2$ for 0.375- and 0.625-inch equivalent-diameter ellipses with axis ratios of 4:1.

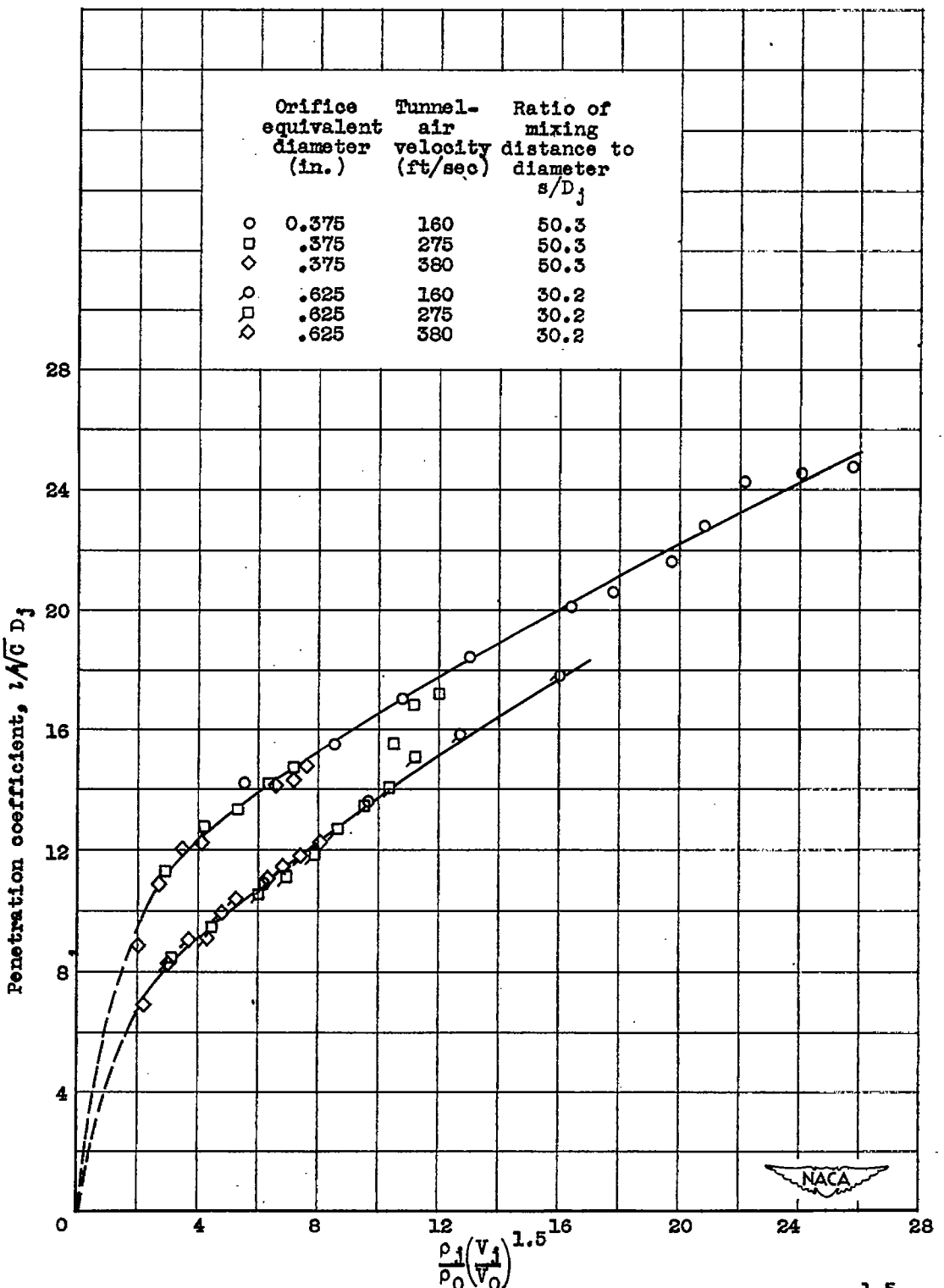

Figure 7. - Variation of penetration coefficient $l/\sqrt{C}\,D_j$ with $\frac{\rho_j}{\rho_0}\left(\frac{V_j}{V_0}\right)^{1.5}$ for 0.375- and 0.625-inch equivalent-diameter ellipses with axis ratios of 2:1.

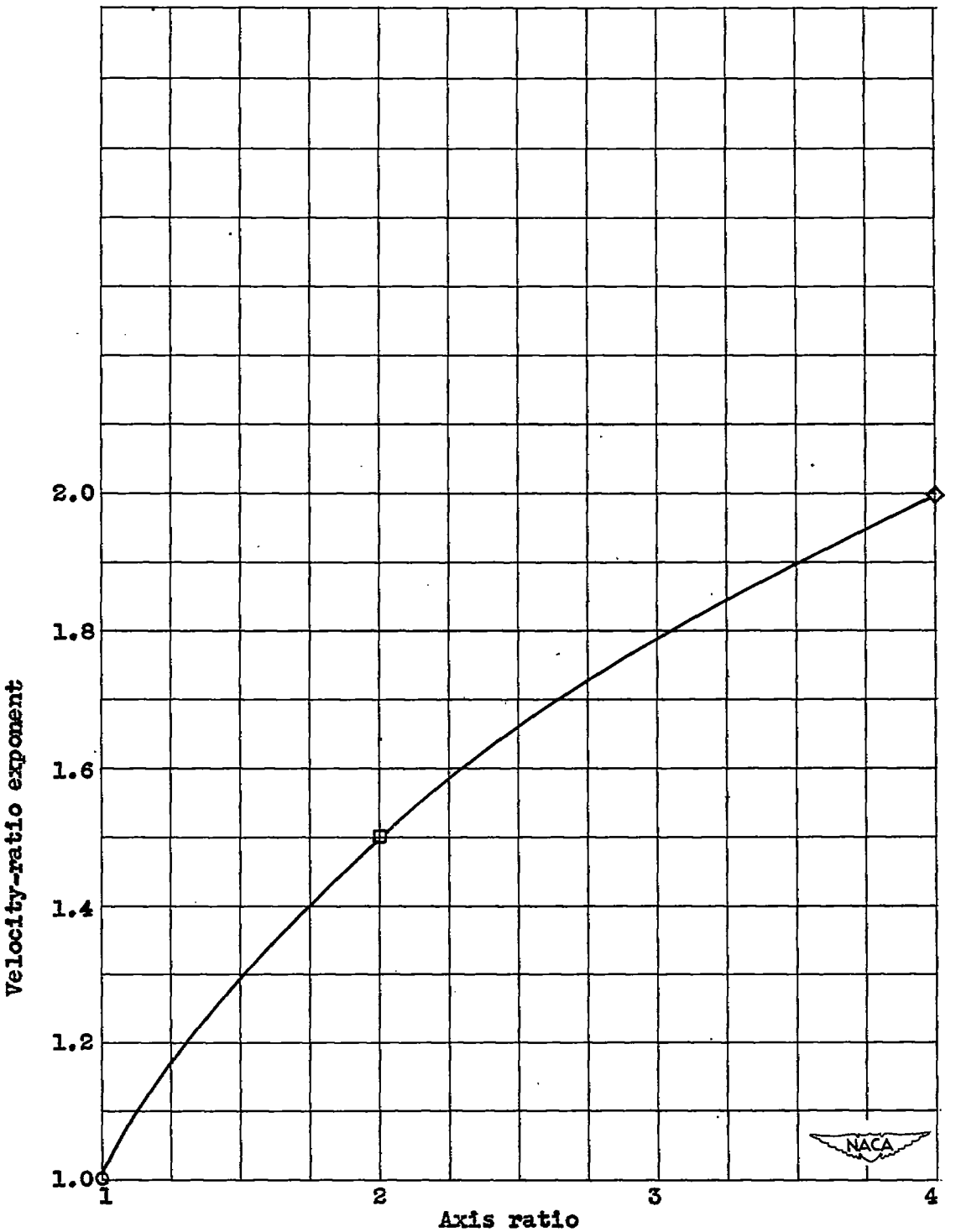

Figure 8. - Variation of velocity-ratio exponent with increasing axis ratio.

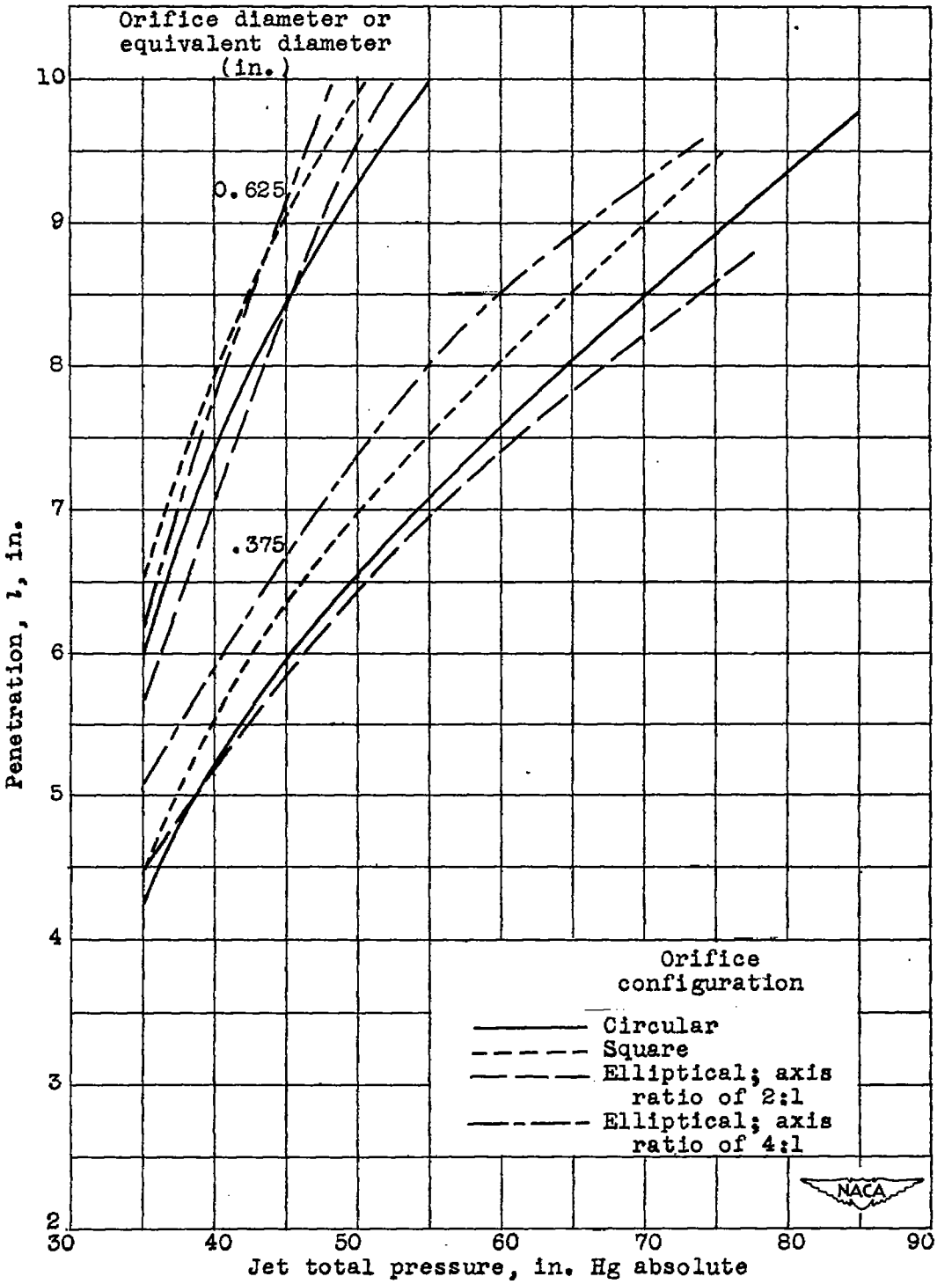

(a) Tunnel-air velocity, 150 feet per second.

Figure 9. - Variation of penetration with jet total pressure for various orifice shapes. Tunnel total pressure, 29.92 inches of mercury; tunnel total temperature, 59° F; jet total temperature, 400° F.

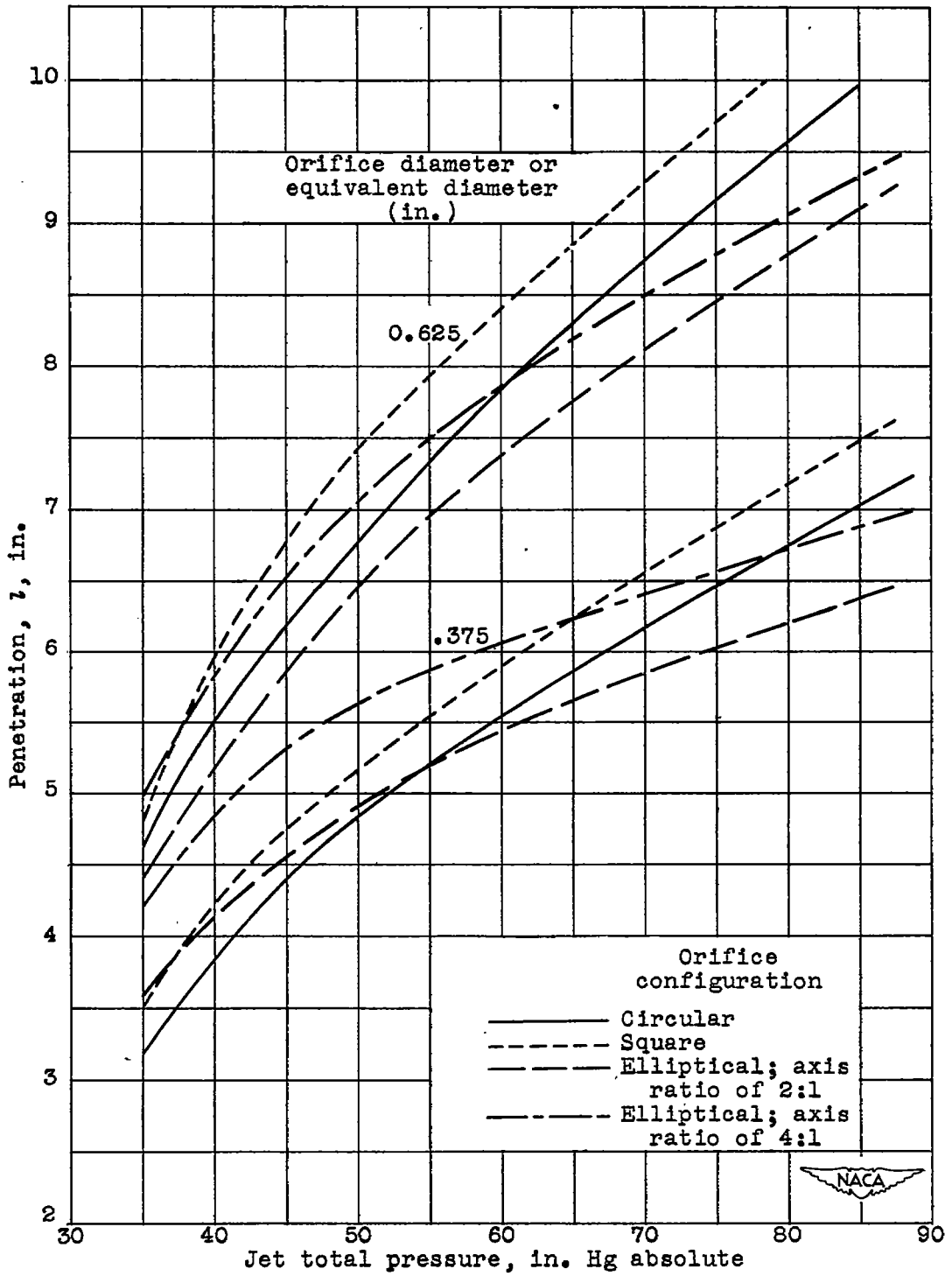

(b) Tunnel-air velocity, 250 feet per second.

Figure 9. - Continued. Variation of penetration with jet total pressure for various orifice shapes. Tunnel total pressure, 29.92 inches of mercury; tunnel total temperature, 59° F; jet total temperature, 400° F.

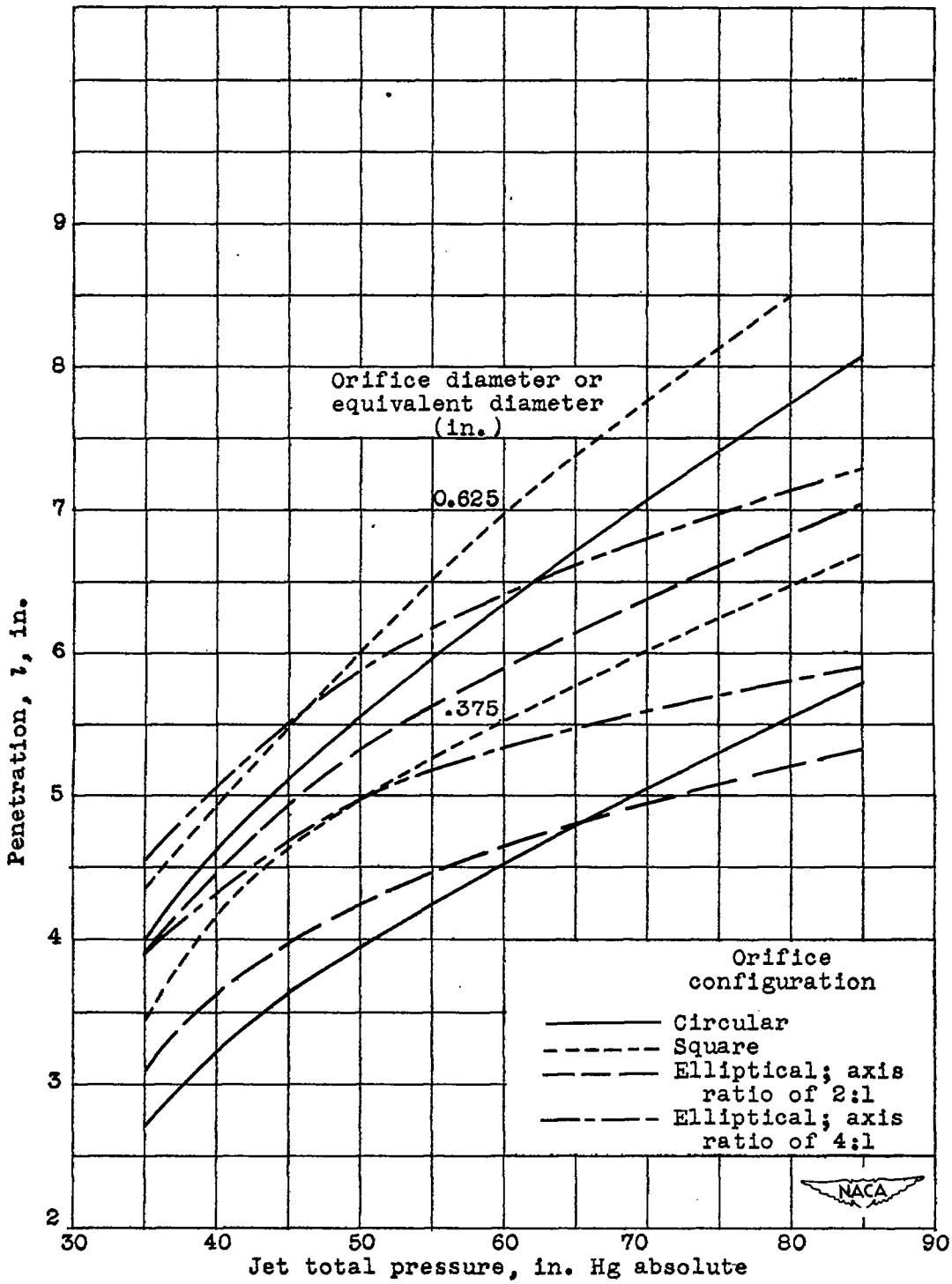

(c) Tunnel-air velocity, 350 feet per second.

Figure 9. - Concluded. Variation of penetration with jet total pressure for various orifice shapes. Tunnel total pressure, 29.92 inches of mercury; tunnel total temperature, 59° F; jet total temperature, 400° F.